*The Canadian Mineralogist*
Vol. 44, pp. 1159-1170 (2006)

# THE CRYSTAL STRUCTURE OF NEAR-END-MEMBER FERROAXINITE FROM AN IRON-CONTAMINATED PEGMATITE AT MALEŠOV, CZECH REPUBLIC

JAN FILIP[§]

*Centre for Nanomaterial Research, Palacky University in Olomouc, Svobody 26, CZ–771 46 Olomouc, Czech Republic*

UWE KOLITSCH

*Department for Mineralogy and Crystallography, University of Vienna – Geocentre, Althanstrasse 14, A–1090 Vienna, Austria*

MILAN NOVÁK

*Institute of Geological Sciences, Masaryk University in Brno, Kotlářská 2, CZ–611 37 Brno, Czech Republic*

OLDŘICH SCHNEEWEISS

*Institute of Physics of Materials, Academy of Sciences of the Czech Republic, Žižkova 22, CZ–616 62 Brno, Czech Republic*

## ABSTRACT

We have characterized ferroaxinite (up to 95 mol.% of end-member composition) from a contaminated granitic pegmatite cutting the magnetite-rich portion of an Fe-skarn body near Malešov, Czech Republic, by means of electron-microprobe analysis, single-crystal X-ray diffraction, infrared spectroscopy and temperature-dependent $^{57}$Fe Mössbauer spectroscopy. The following crystal-chemical formula was obtained: $^{VI}[Ca_{2.00}\ Ca_{2.00}\ (Fe^{2+}_{1.83}Mn_{0.10}Mg_{0.06})_{\Sigma 1.99}\ (Al_{1.97}Fe^{3+}_{0.04})_{\Sigma 2.01}\ Al_{2.00}]\ ^{IV}[B_{2.00}Si_{8.00}]\ O_{30}\ OH_{2.00}$. The crystal structure was refined to $R(F) = 0.0184$ for 4667 observed reflections with $F_o > 4\sigma(F_o)$. We obtained the following unit-cell parameters: $a$ 7.152(1), $b$ 9.206(2), $c$ 8.962(2) Å, $\alpha$ 91.84(3), $\beta$ 98.17(3), $\gamma$ 77.33(3)°, $V$ 569.86(19) Å$^3$. Relative to the other end-members of axinite group, the only significant differences of structural parameters occur at the $Y$ site, where $Fe^{2+}$ atoms predominate; the mean $Y$–O bond length is 2.229 Å. The unusually long Fe–O(14) bond (2.704 Å) of the distorted $Y$ site suggests a [5 + 1] coordination rather than the previously reported distorted [6] coordination for the group. The scarcity of near-end-member ferroaxinite in nature is due to preferred incorporation of Mn into the structure. The formation of near-end-member ferroaxinite in the late stage of pegmatite evolution at Malešov was favored by high activity of Fe, and lack of Mn and Mg in parent low-temperature fluids.

*Keywords*: ferroaxinite, axinite group, electron-microprobe analysis, structure refinement, $^{57}$Fe Mössbauer spectroscopy, granitic pegmatite, Malešov, Czech Republic.

## SOMMAIRE

Nous avons caractérisé la ferroaxinite contenant jusqu'à 95% du pôle, découverte dans une pegmatite granitique contaminée recoupant la portion riche en magnétite d'un skarn près de Malešov, en République Tchèque, au moyen d'analyses à la microsonde électronique, diffraction X sur monocristal, spectroscopie infra-rouge et spectroscopie de Mössbauer $^{57}$Fe à température variable. Nous avons obtenu la formule structurale suivante: $^{VI}[Ca_{2.00}\ Ca_{2.00}\ (Fe^{2+}_{1.83}Mn_{0.10}Mg_{0.06})_{\Sigma 1.99}\ (Al_{1.97}Fe^{3+}_{0.04})_{\Sigma 2.01}\ Al_{2.00}]\ ^{IV}[B_{2.00}Si_{8.00}]\ O_{30}\ OH_{2.00}$. Nous en avons affiné la structure jusqu'à un résidu $R(F)$ de 0.0184 en utilisant 4667 réflexions observées [$F_o > 4\sigma(F_o)$]. Nous obtenons les paramètres réticulaires suivants: $a$ 7.152(1), $b$ 9.206(2), $c$ 8.962(2) Å, $\alpha$ 91.84(3), $\beta$ 98.17(3), $\gamma$ 77.33(3)°, $V$ 569.86(19) Å$^3$. Par rapport aux autres membres du groupe de l'axinite, les seules différences importantes portent sur les paramètres structuraux propres au site $Y$, dans lequel les atomes de $Fe^{2+}$ prédominent; la longueur de liaison $Y$–O moyenne est 2.229 Å. La présence d'une liaison Fe–O(14) anormalement longue (2.704 Å) à ce site difforme indiquerait une coordinence [5 + 1] plutôt que la coordinence [6] attribuée normalement. La rareté de ferroaxinite si rapprochée du pôle serait due à la préférence de cette structure pour le Mn. La formation d'une telle composition de ferroaxinite au stade tardif d'évolution

§ *E-mail address*: filip@sci.muni.cz

de la pegmatite à Malešov est favorisée par l'activité élevée de Fe, et le manque de Mn et de Mg dans la phase fluide circulant à faibles températures.

(Traduit par la Rédaction)

*Mots-clés*: ferroaxinite, groupe de l'axinite, données de microsonde électronique, affinement de la structure, spectroscopie de Mössbauer $^{57}$Fe, pegmatite granitique, Malešov, République Tchèque.

## Introduction

Near-end-member ferroaxinite was found in a granitic pegmatite cutting an iron-rich skarn body at Malešov, near Kutná Hora, Czech Republic. As the previously published descriptions of the structure of ferroaxinite were obtained from samples with only ~80 mol.% of the ferroaxinite component (Swinnea *et al*. 1981, Andreozzi *et al*. 2004), we report here on the result of a crystal-structure refinement of this near-end-member ferroaxinite, supplemented by electron-microprobe analyses, infrared and temperature-dependent Mössbauer spectroscopic studies. We describe the crystal chemistry, crystal structure and probable conditions of formation of ferroaxinite, as well as relationships among end-members of the axinite group.

## Background Information

Minerals of the axinite group typically occur in Ca- and B-rich but relatively Al-poor environments (Pringle & Kawachi 1980, Grew 1996). They have been extensively studied in the past decade (Pieczka & Kraczka 1994, Belokoneva *et al*. 1997, 2001, Fuchs *et al*. 1997, Andreozzi *et al*. 2000a, b, 2004, Salviulo *et al*. 2000, Novák & Filip 2002, Zabinski *et al*. 2002); for a comprehensive list of references to earlier work, see the review of Grew (1996). The general formula, $(CaMn)_4$ $(FeMnMg)_2$ $Al_4$ $B_2$ $Si_8$ $O_{30}$ $(OH)_2$, was proposed by Sanero & Gottardi (1968) and revised by Lumpkin & Ribbe (1979). We use, throughout this work, the site nomenclature according to the generalized structural formula improved by Andreozzi *et al*. (2004): $^{VI}[X(1)$ $X(2)$ $Y$ $Z(1)$ $Z(2)]_2$ $^{IV}[T(1)$ $T(2)$ $T(3)$ $T(4)$ $T(5)]$ $O_{30}$ $(OH)_2$, where VI and IV are coordination numbers; $X(1)$ = Ca (Na), $X(2)$ = Ca ($Mn^{2+}$), $Y$ = $Fe^{2+}$, $Mn^{2+}$, Mg (Zn, $Fe^{3+}$, Al), $Z(1)$ = Al ($Fe^{3+}$), $Z(2)$ = Al, $T(1)$–$T(4)$ = Si and $T(5)$ = B (Si).

The four presently known end-members of the axinite group are classified according to the dominant divalent cation located at the $X$ and $Y$ sites: ferroaxinite, manganaxinite and magnesioaxinite, all with four Ca atoms per formula unit (*apfu*) and dominant Fe, Mn or Mg at the $Y$ site, respectively, and tinzenite with $2 \leq Ca \leq 4$ *apfu* and dominant Mn at both the $X(2)$ and $Y$ sites (Milton *et al*. 1953, Sanero & Gottardi 1968, Basso *et al*. 1973, Lumpkin & Ribbe 1979, Belokoneva *et al*. 2001, Andreozzi *et al*. 2004). Ferroaxinite and Mg-poor manganaxinite are the most common compositions in nature (Grew 1996, Andreozzi *et al*. 2000b); however, no previously reported axinite approached closely the ferroaxinite end-member in composition (Grew 1996, Andreozzi *et al*. 2004, Henry *et al*. 2005).

Manganaxinite and tinzenite occur in metamorphosed Mn-deposits and related rocks, as well as in hydrothermal veins and in some occurrences of granitic pegmatite (Ozaki 1972, Grew 1996, Novák *et al*. 1999). Rare magnesioaxinite is found solely in metamorphic rocks with a high Mg:Fe ratio (Jobbins *et al*. 1975, Andreozzi *et al*. 2000a, Novák & Filip 2002). Ferroaxinite is typical in metamorphic rocks and Alpine veins (Ozaki 1972, Pringle & Kawachi 1980, Grew 1996), but it also occurs in granitic pegmatites (Ozaki 1972, Pieczka & Kraczka 1994, Filip 2002). Ferroaxinite with relatively low Mn and Mg contents is a typical accessory mineral in contaminated pegmatites cutting Fe-skarn bodies in the Moldanubicum, Czech Republic, where it is typically associated with plagioclase ($An_{0–52}$), hastingsite to ferro-edenite, clinozoisite–epidote, Ca-rich schorl to uvite, prehnite, titanite and hedenbergite–diopside (Filip 2002).

## Crystal Structure and Crystal Chemistry of Axinite-Group Minerals

The crystal structure of axinite-group minerals (intermediate composition between ferroaxinite and manganaxinite) was originally proposed by Ito & Takéuchi (1952) and subsequently revised by Ito *et al*. (1969) and Takéuchi *et al*. (1974). The structural details of a member of the manganaxinite–tinzenite solid-solution series were presented by Basso *et al*. (1973), and more recently, the structures of relatively pure manganaxinite and of tinzenite were investigated by Belokoneva *et al*. (1997, 2001), respectively. Ferroaxinite with ~80 mol.% of the end-member component was examined by single-crystal X-ray diffraction by Swinnea *et al*. (1981). Andreozzi *et al*. (2000a) described the structure of near-end-member magnesioaxinite. New structural data for nearly end-member manganaxinite and ferroaxinite with ~80 mol.% of the end-member component were also given by Andreozzi *et al*. (2004).

The crystal structure of axinite (space group $P\bar{1}$) is described as a sequence of layers roughly parallel to $(\bar{1}21)$, containing tetrahedrally and octahedrally coordinated cations. The layer of tetrahedra consist of isolated $B_2$ $Si_8$ $O_{30}$ planar clusters (see Takéuchi *et*

*al*. 1974, Andreozzi *et al*. 2000a), whereas the layer of octahedra is a continuous framework of six-fold Fe(Mn,Mg)–Al–Al–Al–Al–Fe(Mn,Mg) finite chains [*i.e., Y–Z*(1)–*Z*(2)–*Z*(2)–*Z*(1)–*Y*] laterally connected by highly distorted $CaO_6$ octahedra. The existence of the six-membered ring consisting of two disilicate groups [*T*(1) and *T*(2) sites] connected by two $BO_4$ [*T*(5)] tetrahedra is typical of the layer of tetrahedra (Takéuchi *et al*. 1974). The hydrogen atom is located between donor O(16) and acceptor O(13) (Swinnea *et al*. 1981, Belokoneva *et al*. 1997, Andreozzi *et al*. 2000a).

Divalent iron enters exclusively the *Y* site, whereas $Fe^{3+}$ is ordered at both *Z*(1) and, to a lesser extent, also at the *Y* site. The *Z*(2) site, markedly smaller than the *Z*(1) site, is invariably fully occupied by Al (Andreozzi *et al*. 2000a, 2004). In ferroaxinite–manganaxinite solid solutions, an increasing Mn content causes enlargement of the *Y* site and subsequently also of the neighboring *Z*(1) site (Andreozzi *et al*. 2004), thus enabling progressive incorporation of $Fe^{3+}$ into the *Z*(1) site mainly in manganaxinite. In manganaxinite–tinzenite solid-solutions, Mn also enters the smaller *X*(2) site (Basso *et al*. 1973, Andreozzi *et al*. 2000a, 2004), whereas the reported presence of Mn in the larger *X*(1) site (Belokoneva *et al*. 1997, 2001) is rather questionable.

The existence of compositional gaps within the axinite group (Pringle & Kawachi 1980, Grew 1996, Andreozzi *et al*. 2000b, 2004) is believed to be caused by both petrological (scarcity of rocks of appropriate composition, Pringle & Kawachi 1980) and structural factors (Andreozzi *et al*. 2000a, b, 2004, Novák & Filip 2002). Nevertheless, there is an almost linear increase of both unit-cell volume and <*Y*–O> mean distance from magnesioaxinite through ferroaxinite to manganaxinite (Andreozzi *et al*. 2000a, 2004, Salviulo *et al*. 2000).

## Analytical Methods

### *Sample*

The sample of ferroaxinite examined was found in a contaminated granitic pegmatite cutting the magnetite-rich portion of a body of Fe-skarn (grossular–andradite, diopside–hedenbergite and magnetite) at Malešov, near Kutná Hora, Czech Republic (the sample studied is from the mineralogical collection of the Institute of Geochemistry, Mineralogy and Mineral Resources, Faculty of Science, Charles University in Prague, Czech Republic; sample no. 19288). The skarn body is located in the Malín Formation of the Gföhl unit, Kutná Hora crystalline unit, Bohemian Massif (Synek & Oliveriová 1993), representing HP–HT rocks metamorphosed during the polyphase Variscan deformation (Beard *et al*. 1991, Kachlík 1999). The dike of granitic pegmatite, up to 1 m wide, shows a homogeneous internal structure; it is highly contaminated by surrounding iron-rich rocks (magnetite-rich accumulations). The primary minerals of the pegmatite include dominant oligoclase, minor quartz and Fe-rich amphibole (mostly hastingsite). The mineral assemblage with ferroaxinite is developed in small pockets. These formed at the hydrothermal stage, and the following sequence of crystallization was observed: albite → chlorite (Al-bearing chamosite) + calcite I → ferroaxinite + epidote → Fe-rich prehnite + calcite II (Fig. 1). Violet, mostly transparent ferroaxinite forms well-developed isolated axe-shaped crystals (Fig. 1), up to 5 mm in size, with evident striae. Indices of refraction, measured by the immersion method, are: $\alpha$ 1.677(2), $\gamma$ 1.687(2) and $\gamma$–$\alpha$ 0.010.

### *Electron-microprobe analysis and $^{57}$Fe Mössbauer and infrared spectroscopy*

Electron-microprobe analyses (EMPA) were done using a CAMECA SX100 instrument at the Joint Laboratory of Electron Microscopy and Microanalysis, Institute of Geological Sciences, Masaryk University, Brno, and the Czech Geological Survey, Praha, Czech Republic. The following conditions were used: accelerating voltage of 15 keV, sample current of 10 nA, and beam diameter of 5 μm. Augite (Si, Mg), andradite (Ca, Fe), jadeite (Na), almandine (Al), rhodonite (Mn), synthetic $TiO_2$ (Ti) and chromite (Cr) were used as standards. Data were reduced using the X-phi routine (Merlet 1994). Chemical formulae of ferroaxinite were calculated on the basis of 32 anions and from the assumed stoichiometry B = 2, OH = 2 *apfu*.

The $^{57}$Fe transmission Mössbauer spectra of a powdered sample of ferroaxinite were accumulated in constant-acceleration mode using a $^{57}$Co-in-Rh source and a 1024-channel detector at room temperature (RT) and at low temperatures (LT), at both 80 K and 25 K. With respect to the strongly overlapped doublets in axinite spectra (*cf*. Fuchs *et al*. 1997, Andreozzi *et al*.

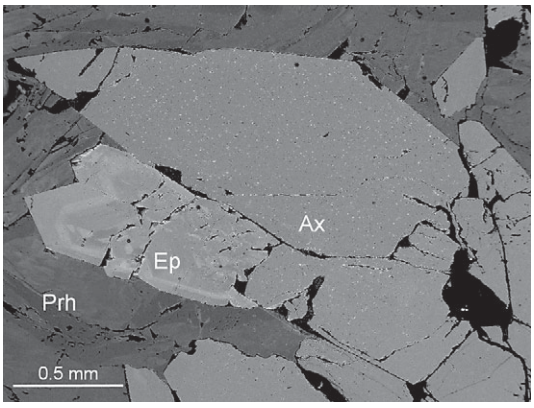


FIG. 1. BSE image of near-end-member ferroaxinite (Ax) from Malešov (Prh: Fe-rich prehnite, Ep: Fe-rich epidote).

2004), we also applied RT $^{57}$Fe Mössbauer spectroscopy with resonant detection of gamma rays using the moving sample to get narrower spectral lines and a better signal-to-noise ratio than in conventional $^{57}$Fe Mössbauer spectrometers (see Mashlan *et al*. 2004). Spectra were fitted by Lorentz functions using the computer program CONFIT2000, v. 4.2.3 (Žák 2001). The isomer shift was calibrated with regard to an α-Fe foil. The percentages of the $Fe^{2+}$ and $Fe^{3+}$ contents were established by measuring the integrated area of the respective doublets in the 25 K spectrum (see McCammon 2004).

A Fourier-transform infrared (FTIR) absorption spectrum of ferroaxinite was recorded in the 4000–400 $cm^{-1}$ spectral region using a Perkin Elmer FTIR 1760X spectrometer equipped with a TGS detector. The sample was prepared by mixing 1 mg of powdered sample with 300 mg of KBr (dried before hand at 120°C) and pressing in an evacuated die at 10 tonnes. A total of 128 scans were done in air with a resolution of 4 $cm^{-1}$.

TABLE 1. SINGLE-CRYSTAL X-RAY DATA, DATA COLLECTION AND DETAILS OF STRUCTURE-REFINEMENT FOR NEAR-END-MEMBER FERROAXINITE FROM MALEŠOV

**Crystal data**

| | | | |
|---|---|---|---|
| *a* (Å) | 7.152(1) | Space group | P1 |
| *b* (Å) | 9.206(2) | *Z* | 2 |
| *c* (Å) | 8.962(2) | F (000) | 562 |
| α (°) | 91.84(3) | $\rho_{calc}$ (g cm$^{-3}$) | 3.312 |
| β (°) | 98.17(3) | μ (mm$^{-1}$) | 2.841 |
| γ (°) | 77.33(3) | | |
| *V* (Å$^3$) | 569.86(19) | | |
| Crystal dimensions (mm) | | 0.27 × 0.20 × 0.13 | |

**Data collection and processing**

Single-crystal four-circle diffractometer Nonius Kappa CCD, Mo tube, graphite monochromator, capillary-optics collimator 300 μm in diameter, program COLLECT (Nonius 2004), scan mode: φ and ω scans, frame width = 2°, crystal-to-detector distance 30 mm, $2\theta_{max}$ = 70°, *T* = 293 K, Nonius program suite DENZO-SMN (Otwinowski & Minor 1997), corrections for Lorentz, polarization and background; absorption was corrected according to the multi-scan method (Otwinowski & Minor 1997, Otwinowski *et al*. 2003).

| | |
|---|---|
| Total number of frames | 603 |
| Collection time per degree (s) | 10 |
| *h*, *k*, *l* ranges | -11→11, -14→14, -14→14 |
| Total reflections collected | 9923 |
| Unique reflections | 5012 |
| $R_{int} = \Sigma \lvert F_o^2 - F_o^2(\text{mean}) \rvert / \Sigma F_o^2$ | 0.0148 |
| "Observed" reflections, $F_o > 4\sigma(F_o)$ | 4667 |

**Refinement**

Full-matrix least-squares on $F^2$, program SHELXL-97 (Sheldrick 1997); 242 variable parameters (p), $\Delta/\sigma$ = 0.001

| | |
|---|---|
| *R*1(*F*) for "observed" reflections | 0.0184 |
| *wR*2($F^2$)[b] for all reflections | 0.0513 |
| Extinction coefficient | 0.0348(10) |
| a, b[c] | 0.02, 0.33 |
| GooF = $\{\Sigma [w(F_o^2 - F_c^2)^2] / (n - p)\}^{0.5}$ | 1.093 |
| $\Delta\rho_{max}$, $\Delta\rho_{min}$, (e/Å$^3$) | 0.47, -0.53 |

[b] $R1(F) = \Sigma(\lvert F_o \rvert - \lvert F_c \rvert) / \Sigma F_o$; $wR2(F^2) = [\Sigma w(F_o^2 - F_c^2)^2 / \Sigma wF_o^4]^{1/2}$.
[c] $w = 1 / [\sigma^2(F_o^2) + [a*P]^2 + [b*P]]$, $P = [\max(0, F_o^2)] + 2*F_c^2) / 3]$.

*X-ray-diffraction experiments and crystal-structure refinement*

Data for structure refinement (SREF) were collected with an automatic four-circle single-crystal X-ray diffractometer equipped with a CCD area detector (Nonius Kappa CCD; Mo*K*α radiation, λ = 0.71073 Å) and with a 300-μm diameter capillary-optics collimator to provide better resolution. For the collection of intensity data, a suitable fragment of a very good quality and with the approximate dimensions 0.13 × 0.20 × 0.27 mm was cut and mounted on a glass fiber. A full sphere of diffraction data up to 2θ = 70° was collected (see Table 1 for details). The intensity data were processed with the Nonius program suite DENZO–SMN, corrected for Lorentz, polarization, absorption and background effects.

The positional parameters for magnesioaxinite given by Andreozzi *et al*. (2000a) were used as starting parameters for a full-matrix least-squares refinement using SHELXL97 (Sheldrick 1997). For easier comparison with the previously published data on axinite-group minerals, we adopted the cell orientation recommended by Peacock (1937), best representing the unique set defined by the Eisenstein-reduced lattice (see Andreozzi *et al*. 2000a, Salviulo *et al*. 2000). The final steps of the refinement resulted in w*R*2($F^2$) = 0.0513 for the 5012 unique reflections, and *R*1(*F*) = 0.0184 for the 4667 observed reflections. Relevant information on crystal data, data collection, and refinements is given in Table 1. Polyhedron-distortion parameters and polyhedron volumes were calculated by using of the Geometri software (kindly provided by G.B. Andreozzi).

## RESULTS

*Crystal chemistry: EMPA, $^{57}$Fe Mössbauer and FTIR spectroscopy*

The ferroaxinite from Malešov is chemically homogeneous in the BSE image (Fig. 1). Its chemical composition is very close to the ideal stoichiometry: 7.95 < Si < 8.05 (8.01), 3.92 < Al < 4.01 (3.97) and 3.95 < Ca < 4.04 (3.99) (all in *apfu*; Table 2). The *Y* site is occupied by dominant $Fe^{2+}$, between 1.77 and 1.95 (1.83) *apfu* (from a combination of EMPA and Mössbauer spectroscopy; Table 2) and by minor to negligible amounts of Mn, between 0.06 and 0.14 (0.10) *apfu* and between 0.03 and 0.09 Mg (0.06) *apfu*. These proportions are relatively constant in all analyzed crystals (Fig. 2). Hence, this sample represents nearly ideal ferroaxinite, $(Ca)_4\ (Fe)_2\ Al_4\ B_2\ Si_8\ O_{30}\ (OH)_2$ (up to 95 mol.%, Fig. 2), and it is the purest sample described to date (*cf*. Grew 1996, Andreozzi *et al*. 2000b, Henry *et al*. 2005). Minor to trace amounts of $Fe^{3+}$ (0.04 *apfu*, established from a combination of EMPA, SREF and Mössbauer spectroscopy), and negligible Ti, Cr and Na (less than 0.01 *apfu*) were found. The stoichiometric

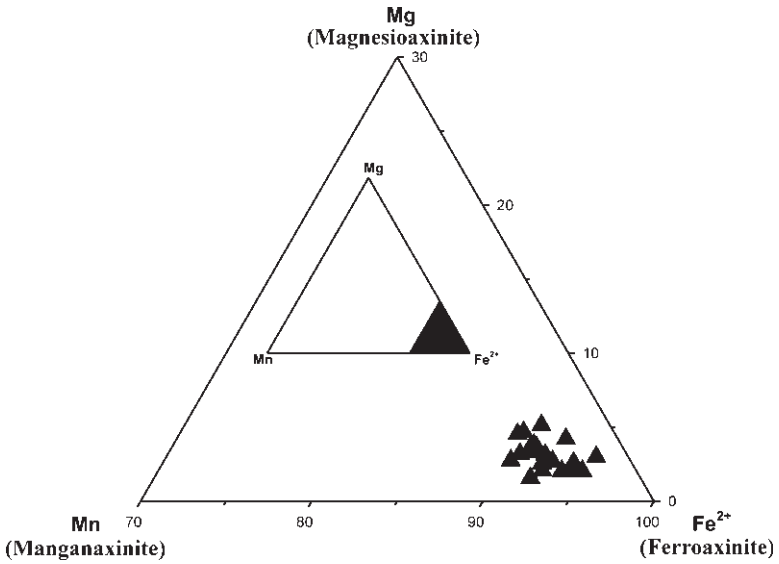


FIG. 2. Composition of ferroaxinite from Malešov in the Mn–Mg–$Fe^{2+}_{tot}$ triangle.

content of boron was confirmed from the *T*(5)-site volume calculated from SREF results, in agreement with results of Andreozzi *et al.* (2000b) (see the next section). Chemical compositions of selected associated minerals also are given in Table 2.

The $^{57}$Fe Mössbauer spectra of ferroaxinite from Malešov (Fig. 3) are very similar to those of ferroaxinite published in the literature (*cf.* Fuchs *et al.* 1997, Andreozzi *et al.* 2004). They are simpler than the spectrum published by Pieczka & Kraczka (1994) and Zabinski *et al.* (2002) for ferroaxinite from Strzegom, Poland, where rather unusual substitutions were described. However, their sample obviously contained impurities of associated epidote (unpublished data of J. Filip). Our Mössbauer spectra were fitted with two strongly overlapped doublets of quadrupole splitting (Fig. 3). The Mössbauer parameters refined at RT are: isomer shifts (δ): 1.14 and 0.22 mm/s, and quadrupole splitting ($\Delta E_Q$): 2.11 and 0.38 mm/s (0.56 mm/s in case of resonant spectra), respectively. The Mössbauer parameters at LT are: δ = 1.27 and 0.32 mm/s, and $\Delta E_Q$ = 2.58 and 0.44 mm/s, respectively. According to the existing literature and results from SREF and EMPA, the two doublets were attributed to $^{Y}Fe^{2+}$ and $^{Z1}Fe^{3+}$. The δ values are typical of high-spin $Fe^{2+}$ and $Fe^{3+}$, and are within the range for octahedrally coordinated iron in common silicates (*cf.* Gonser 1975, Dyar *et al.* 1998, McCammon 2004). The relative areas of absorption in the LT (25 K) spectra are 98% for $Fe^{2+}$ and 2% for $Fe^{3+}$.

The FTIR spectrum (Fig. 4) reflects the great complexity of the axinite structure. The large number of sharp bands in the 1200 to 400 $cm^{-1}$ spectral region, corresponding to fundamental Si–O, B–O, Al–O, and Fe–O vibrations, cannot be assigned without uncertainty. Nevertheless, this part of the spectrum is comparable to FTIR spectra of other axinite-group minerals, with no significant differences (*e.g.*, Fuchs *et al.* 1997). The spectrum in the OH-stretching frequency region consists of a sharp (FWHM ~40 $cm^{-1}$) absorption band at 3382 $cm^{-1}$ (Fig. 4) caused by the stretching vibration of the O(16)–H group bonded to O(13). The evident asymmetry of this band (Fig. 4) may imply a slight disorder of the hydrogen bond within the ferroaxinite structure, reflecting substitutions at the coordinating sites (*e.g.*, $Fe^{3+}$-for-Al). The adjacent small and broad band at around 3485 $cm^{-1}$ indicates a stretching mode of another O–H bond in the ferroaxinite structure. The high background in the 3000 to 3700 $cm^{-1}$ spectral region and the weakly pronounced band at *ca.* 1600 $cm^{-1}$, typical of the $H_2O$-bending mode, indicate the presence of free water in fluid inclusions (if water adsorbed on the powdered sample is excluded).

*Crystal structure*

The unit-cell parameters obtained from SREF (Table 1) are close to the published values for most samples of ferroaxinite. The final coordinates (Table 3) are close to those previously reported for other axinite structures (*cf.* Swinnea *et al.* 1981, Belokoneva *et al.* 1997, Andreozzi *et al.* 2000a, 2004). The complete table of structure factors is available from the Depository of Unpublished Data, CISTI, National Research

TABLE 2. REPRESENTATIVE CHEMICAL COMPOSITIONS OF FERROAXINITE AND OF ACCOMPANYING MINERALS FROM PEGMATITE AT MALEŠOV

| | 1 | 2 | 3 | 4 | 5 | 6 | 7 | 8 | 9 | 10 |
|---|---|---|---|---|---|---|---|---|---|---|
| $SiO_2$ wt% | 42.24 | 42.18 | 41.66 | 42.21 | 42.24 | 42.13 | 38.02 | 22.31 | 42.74 | 69.18 |
| $TiO_2$ | 0.04 | 0.01 | 0.04 | 0.01 | 0.00 | 0.00 | 0.02 | 0.07 | 0.02 | 0.02 |
| $Al_2O_3$ | 17.70 | 17.61 | 17.38 | 17.93 | 17.97 | 17.81 | 25.21 | 20.16 | 20.61 | 19.76 |
| $Cr_2O_3$ | 0.02 | 0.01 | 0.00 | 0.00 | 0.00 | 0.01 | 0.01 | 0.02 | 0.00 | 0.02 |
| CaO | 19.52 | 19.70 | 19.67 | 19.52 | 19.81 | 19.49 | 22.89 | 0.00 | 26.27 | 0.06 |
| MgO | 0.33 | 0.11 | 0.19 | 0.23 | 0.15 | 0.14 | 0.00 | 1.12 | 0.00 | 0.01 |
| FeO * | 11.58 | 11.63 | 12.42 | 11.59 | 11.91 | 11.77 | n.d. | 45.69 | n.d. | n.d. |
| $Fe_2O_3$ ** | n.d. | n.d. | n.d. | n.d. | n.d. | n.d. | 11.56 | n.d. | 5.43 | n.d. |
| MnO | 0.65 | 0.78 | 0.43 | 0.68 | 0.47 | 0.53 | 0.04 | 0.31 | 0.01 | n.d. |
| $Na_2O$ | 0.01 | 0.00 | 0.00 | 0.00 | 0.00 | 0.00 | 0.00 | 0.00 | 0.01 | 12.20 |
| $B_2O_3$ [a] | 6.10 | 6.09 | 6.05 | 6.11 | 6.13 | 6.09 | - | - | - | - |
| $H_2O$ [a] | 1.58 | 1.58 | 1.57 | 1.58 | 1.59 | 1.58 | 1.90 | 10.33 | 4.26 | - |
| Total | 99.77 | 99.70 | 99.43 | 99.88 | 100.26 | 99.54 | 99.65 | 100.01 | 99.34 | 101.25 |
| FeO [b] | 11.35 | 11.40 | 12.17 | 11.36 | 11.67 | 11.53 | - | - | - | - |
| $Fe_2O_3$ [b] | 0.26 | 0.26 | 0.28 | 0.26 | 0.26 | 0.26 | - | - | - | - |
| Si *apfu* | 8.018 | 8.025 | 7.977 | 8.003 | 7.988 | 8.017 | 3.003 | 2.591 | 3.009 | 2.987 |
| Ti | 0.006 | 0.001 | 0.006 | 0.001 | 0.000 | 0.000 | 0.001 | 0.006 | 0.001 | 0.001 |
| Al | 3.960 | 3.949 | 3.922 | 4.007 | 4.005 | 3.994 | 2.347 | 2.760 | 1.709 | 1.006 |
| Cr | 0.003 | 0.002 | 0.000 | 0.000 | 0.000 | 0.002 | 0.001 | 0.002 | 0.000 | 0.001 |
| Ca | 3.970 | 4.016 | 4.035 | 3.966 | 4.014 | 3.974 | 1.937 | 0.000 | 1.982 | 0.003 |
| Mg | 0.093 | 0.031 | 0.054 | 0.065 | 0.042 | 0.040 | 0.000 | 0.194 | 0.000 | 0.001 |
| $Fe^{2+}$ [b] | 1.801 | 1.813 | 1.949 | 1.801 | 1.846 | 1.836 | - | 4.438 | - | - |
| $Fe^{3+}$ [b] | 0.037 | 0.037 | 0.040 | 0.037 | 0.038 | 0.037 | 0.687 | - | 0.289 | - |
| $Mn^{2+}$ | 0.105 | 0.126 | 0.070 | 0.109 | 0.075 | 0.085 | 0.003 | 0.030 | 0.000 | - |
| Na | 0.004 | 0.000 | 0.000 | 0.000 | 0.000 | 0.000 | 0.000 | 0.000 | 0.002 | 1.021 |
| B | 2.000 | 2.000 | 2.000 | 2.000 | 2.000 | 2.000 | - | - | - | - |
| H | 2.000 | 2.000 | 2.000 | 2.000 | 2.000 | 2.000 | 1.000 | 8.000 | 2.000 | - |
| Σ cations | 19.997 | 19.999 | 20.058 | 19.994 | 20.009 | 19.985 | 7.979 | 10.022 | 6.992 | 5.019 |

* All Fe expressed as FeO. ** All Fe expressed as $Fe_2O_3$. [a] Calculated from stoichiometry. [b] Determined by Mössbauer spectroscopy. n.d.: not determined. Columns: 1–6 axinite, 7 Fe-rich epidote, 8 chamosite, 9 Fe-rich prehnite, 10 albite.

Council, Ottawa, Ontario K1A 0S2, Canada. Selected bond-distances for tetrahedral and octahedral sites are presented in Table 4, along with calculated site-volumes and values of indices of deformation of the coordination polyhedra, for example the mean quadratic elongation (λ) and the angular variance ($\sigma^2$), as defined by Robinson *et al*. (1971). As the overall structural features of ferroaxinite (Table 4) are comparable to those of magnesioaxinite and manganaxinite (tinzenite), described in detail by Andreozzi *et al*. (2000a) and Belokoneva *et al*. (1997, 2001), our discussion will focus on the interesting differences (see Discussion).

The SREF indicates complete occupancy of the *T*(1) to *T*(4) sites by Si, of the *X*(1) and *X*(2) by Ca, and of *Z*(2) by Al. Hence, $Fe^{3+}$-for-Si, Al-for-Si and B-for-Si substitutions (*cf*. Andreozzi *et al*. 2000a, 2004) are unlikely, and the tinzenite component, according to the vector $MnCa_{-1}$, is present to a negligible extent only. At the *Y* site, the longest *Y*–O(14) bond amounts to 2.704 Å, and the second longest *Y*–O(6) bond is 2.372 Å (Table 4). The mean distance of the remaining four bonds is 2.075 Å. The *Z*(1) site, with refined occupancy $Al_{0.9837(19)}Fe_{0.0163(19)}$ (Table 3), is the center of an almost regular octahedron (λ = 1.006 and $\sigma^2$ = 19.4), with mean <*Z*(1)–O> = 1.911 Å. The volume of this site (9.216 $Å^3$) is 0.170 $Å^3$ larger than that of the *Z*(2) site (Table 4), occupied solely by Al.

The volume of the *T*(5) site (1.671 $Å^3$) as well as the values of both distortion parameters (λ = 1.006, $\sigma^2$ = 25.15) suggest full occupancy of the *T*(5) site by boron in the ferroaxinite from Malešov. In fact, these values compare well with the respective values of the *T*(5) site in magnesioaxinite (*cf*. Andreozzi *et al*. 2000a). Moreover, for the axinite group, a *T*(5)-site volume of *ca*. 1.675 $Å^3$ was found to be characteristic, and indicative of full occupancy by boron (*cf*. Andreozzi *et al*. 2000b).

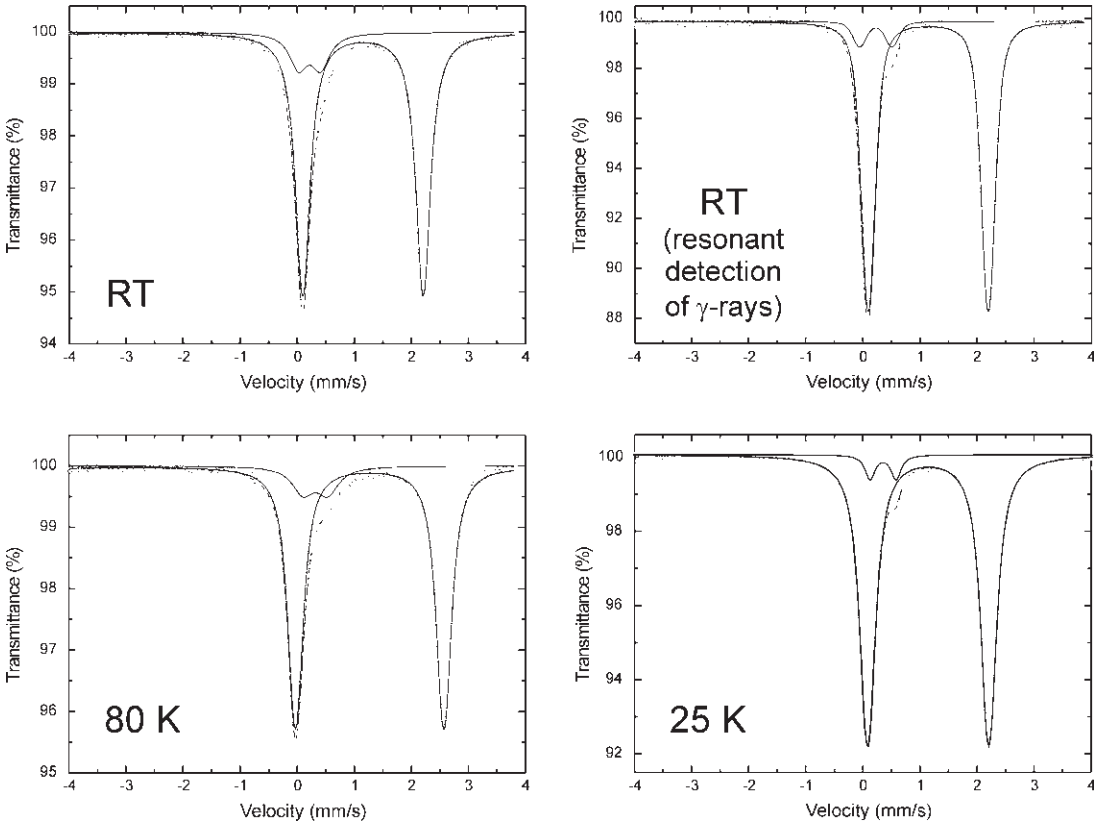


FIG. 3. Mössbauer spectra of ferroaxinite from Malešov. The two doublets indicate major $Fe^{2+}$ and minor $Fe^{3+}$ (see text).

## DISCUSSION

### *Chemical composition of ferroaxinite and mechanisms of substitution*

The chemical composition of ferroaxinite from Malešov is very close to end-member ferroaxinite. It has the following crystal-chemical formula derived from EMPA, $^{57}$Fe Mössbauer spectroscopy and SREF data: $^{VI}[Ca_{2.00}\ Ca_{2.00}\ (Fe^{2+}_{1.83}Mn_{0.10}Mg_{0.06})_{\Sigma 1.99}\ (Al_{1.97}Fe^{3+}_{0.04})_{\Sigma 2.01}\ Al_{2.00}]\ ^{IV}[B_{2.00}Si_{8.00}]\ O_{30}\ OH_{2.00}$. The structurally refined Al:Fe ratio, $Al_{0.9837(19)}Fe_{0.0163(19)}$ at the *Z*(1) site, is in good agreement with the small $Fe^{3+}$ content deduced from the 25 K Mössbauer spectrum (2% $Fe_{tot}$, Al:Fe ratio of $Al_{0.981}Fe_{0.019}$; *cf.* Table 2). Consequently, the homovalent exchange-vectors observed are: minor $MnFe^{2+}_{-1}$ and $MgFe^{2+}_{-1}$, and negligible $Fe^{3+}Al^{3+}_{-1}$. No $Fe^{3+}$ was detected at the *Z*(2) and *Y* sites or in any of tetrahedral sites.

### *Structure refinement*

The previously published refinements of the ferroaxinite structure are based on samples containing relatively high concentrations of Mg (0.21 and 0.30 *apfu*), but relatively low Mn (0.15 and 0.06 *apfu*; Swinnea *et al.* 1981, Andreozzi *et al.* 2004, respectively). Thus, structural parameters derived from those samples are clearly controlled by the presence of these cations, invariably located at the *Y* site. The unit-cell parameters of near-end-member ferroaxinite from Malešov (Table 1) are intermediate between those of magnesioaxinite (smaller parameters; *cf.* Andreozzi *et al.* 2000a) and manganaxinite (larger parameters; *cf.* Belokoneva *et al.* 1997). This is in agreement with the results of Salviulo *et al.* (2000), who demonstrated the differences in powder-diffraction data among end-members of the axinite group; according to Vegard's law, these reflect the different ionic radii of the octahedrally coordinated divalent cations present at the *Y* site (Mg: 0.72 Å, Fe: 0.78 Å, Mn: 0.83 Å; Shannon 1976).

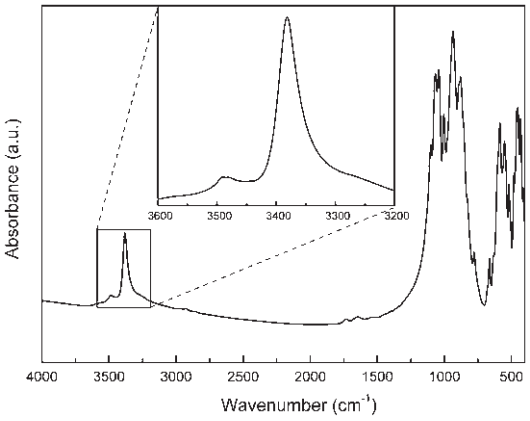


FIG. 4. FTIR spectrum of ferroaxinite from Malešov. The ripples at ~2900 $cm^{-1}$ are due to impurities of organic matter.

Compared to the magnesioaxinite end-member (Andreozzi *et al*. 2000a), the mean *Y*–O distance (2.229 Å) and polyhedron volume at the *Y* site (13.305 $Å^3$) of near-end-member ferroaxinite are markedly larger than those of the Mg end-member (Andreozzi *et al*. 2000a). Similarly, there is markedly increasing deformation of the $YO_6$ polyhedron from magnesioaxinite to ferroaxinite, reflected by an increase in the $\sigma^2$ value from 177.7 (Andreozzi *et al*. 2000a) to 224 (this work). The negligible changes in the bond distances and distortion parameters of the remaining octahedra, and particularly the tetrahedra, are comparable to those of axinite-group phases of various compositions (*cf*. Andreozzi *et al*. 2000a *versus* Table 4).

In accordance with previous studies of the axinite structure (*e.g.,* Belokoneva *et al*. 1997, Andreozzi *et al*. 2000a), the indices of deformation of the *Z*(1) and *Z*(2) coordination polyhedra, *i.e.,* λ and $\sigma^2$ (Table 4), indicate almost regular octahedra. In excellent agreement with SREF, the Mössbauer parameters of $Fe^{3+}$ (δ and $\Delta E_Q$, see previous section), interpreted above as due to substitution of $Fe^{3+}$ for Al at the *Z*(1) site, indicate a low distortion of the *Z*(1) site (*cf*. McCammon 2004).

TABLE 3. ATOM COORDINATES AND EQUIVALENT ISOTROPIC ($U_{eq}$) AND ANISOTROPIC DISPLACEMENT PARAMETERS ($Å^2$) FOR NEAR-END-MEMBER FERROAXINITE FROM MALEŠOV

| Atom | *x* | *y* | *z* | $U_{eq}$ | $U_{11}$ | $U_{22}$ | $U_{33}$ | $U_{23}$ | $U_{13}$ | $U_{12}$ |
|---|---|---|---|---|---|---|---|---|---|---|
| *T*(1) | 0.21024(4) | 0.44997(3) | 0.23430(3) | 0.00447(5) | 0.00501(11) | 0.00399(11) | 0.00438(12) | 0.00039(8) | 0.00035(9) | -0.00106(9) |
| *T*(2) | 0.21917(4) | 0.27475(3) | 0.52333(3) | 0.00379(5) | 0.00349(11) | 0.00387(11) | 0.00406(11) | 0.00019(8) | 0.00036(8) | -0.00101(8) |
| *T*(3) | 0.69820(4) | 0.25644(3) | 0.01151(3) | 0.00459(6) | 0.00519(11) | 0.00459(11) | 0.00374(11) | 0.00040(8) | 0.00070(8) | -0.00041(9) |
| *T*(4) | 0.64140(4) | 0.01946(3) | 0.23044(3) | 0.00413(5) | 0.00392(11) | 0.00491(11) | 0.00372(11) | 0.00019(8) | 0.00077(8) | -0.00115(9) |
| *T*(5) | 0.46146(16) | 0.63436(12) | 0.28684(12) | 0.00474(17) | 0.0046(4) | 0.0049(4) | 0.0047(4) | -0.0004(3) | 0.0008(3) | -0.0009(3) |
| *Z*(1)* | 0.05241(4) | 0.80071(3) | 0.25398(2) | 0.00379(9) | 0.00382(14) | 0.00396(14) | 0.00362(15) | 0.00019(9) | 0.00061(9) | -0.00084(9) |
| *Z*(2) | 0.35207(4) | 0.93593(3) | 0.42115(4) | 0.00415(6) | 0.00418(12) | 0.00429(13) | 0.00414(13) | -0.00033(10) | 0.00059(10) | -0.00133(10) |
| *Y** | 0.76793(2) | 0.590928(19) | 0.111915(19) | 0.00825(5) | 0.00543(8) | 0.01147(8) | 0.00813(8) | 0.00305(5) | 0.00081(5) | -0.00209(5) |
| *X*(1) | 0.74654(3) | 0.34815(2) | 0.39531(2) | 0.00780(5) | 0.00888(9) | 0.00599(8) | 0.00774(9) | 0.00133(6) | -0.00066(6) | -0.00090(6) |
| *X*(2) | 0.18294(3) | 0.10007(2) | 0.08383(2) | 0.00845(5) | 0.00941(9) | 0.00784(9) | 0.00767(9) | 0.00229(6) | -0.00257(7) | -0.00303(7) |
| O(1) | 0.05360(11) | 0.60321(8) | 0.18957(9) | 0.00670(13) | 0.0068(3) | 0.0049(3) | 0.0078(3) | 0.0002(2) | -0.0002(2) | -0.0006(2) |
| O(2) | 0.23119(12) | 0.33833(9) | 0.09578(9) | 0.00882(14) | 0.0116(3) | 0.0072(3) | 0.0077(3) | -0.0021(2) | 0.0018(3) | -0.0019(3) |
| O(3) | 0.41844(11) | 0.48704(8) | 0.31215(9) | 0.00670(13) | 0.0055(3) | 0.0053(3) | 0.0095(3) | 0.0013(2) | -0.0005(2) | -0.0023(2) |
| O(4) | 0.13537(12) | 0.37210(9) | 0.36980(9) | 0.00996(14) | 0.0083(3) | 0.0132(4) | 0.0087(3) | 0.0062(3) | -0.0003(3) | -0.0032(3) |
| O(5) | 0.02163(11) | 0.24270(9) | 0.56436(9) | 0.00626(13) | 0.0051(3) | 0.0087(3) | 0.0057(3) | 0.0009(2) | 0.0014(2) | -0.0026(2) |
| O(6) | 0.32702(11) | 0.38060(8) | 0.64393(9) | 0.00649(13) | 0.0048(3) | 0.0061(3) | 0.0081(3) | -0.0019(2) | -0.0005(2) | -0.0015(2) |
| O(7) | 0.38056(11) | 0.12747(8) | 0.49578(9) | 0.00539(12) | 0.0046(3) | 0.0045(3) | 0.0067(3) | -0.0014(2) | 0.0005(2) | -0.0006(2) |
| O(8) | 0.53476(11) | 0.34395(9) | 0.87689(9) | 0.00692(13) | 0.0072(3) | 0.0080(3) | 0.0048(3) | 0.0014(2) | 0.0014(2) | 0.0007(2) |
| O(9) | 0.87563(11) | 0.15555(8) | 0.93367(9) | 0.00590(12) | 0.0057(3) | 0.0061(3) | 0.0055(3) | -0.0002(2) | 0.0017(2) | -0.0001(2) |
| O(10) | 0.76780(12) | 0.36672(9) | 0.13914(9) | 0.00874(14) | 0.0113(3) | 0.0081(3) | 0.0068(3) | -0.0017(2) | 0.0006(3) | -0.0028(3) |
| O(11) | 0.60268(12) | 0.13512(9) | 0.08713(9) | 0.00901(14) | 0.0100(3) | 0.0099(3) | 0.0078(3) | 0.0044(3) | 0.0009(3) | -0.0032(3) |
| O(12) | 0.43624(11) | 0.98117(9) | 0.24413(8) | 0.00590(12) | 0.0048(3) | 0.0086(3) | 0.0051(3) | 0.0007(2) | 0.0011(2) | -0.0027(2) |
| O(13) | 0.72081(11) | 0.10006(9) | 0.38469(8) | 0.00604(12) | 0.0070(3) | 0.0071(3) | 0.0045(3) | -0.0010(2) | 0.0008(2) | -0.0027(2) |
| O(14) | 0.79432(11) | 0.87507(9) | 0.17743(9) | 0.00700(13) | 0.0050(3) | 0.0081(3) | 0.0067(3) | -0.0011(2) | 0.0003(2) | 0.0008(2) |
| O(15) | 0.32502(11) | 0.74622(8) | 0.35434(8) | 0.00497(12) | 0.0046(3) | 0.0047(3) | 0.0057(3) | -0.0011(2) | 0.0011(2) | -0.0008(2) |
| O(16) | 0.09682(11) | 0.99539(8) | 0.32260(9) | 0.00578(13) | 0.0047(3) | 0.0062(3) | 0.0064(3) | -0.0009(2) | 0.0014(2) | -0.0007(2) |
| H | 0.993(3) | 0.963(2) | 0.631(2) | 0.021(5)** | | | | | | |

* Refined occupancy ratios for *Z*(1): $Al_{0.9837(19)}Fe_{0.0163(19)}$; for *Y*: $Fe_{0.9413(19)}Mg_{0.0587(19)}$. ** Isotropic refinement $U_{iso}$.

TABLE 4. BOND LENGTHS (Å) FOR THE OCTAHEDRALLY AND TETRAHEDRALLY COORDINATED SITES OF FERROAXINITE FROM MALEŠOV

| | | | | | | | | | | | |
|---|---|---|---|---|---|---|---|---|---|---|---|
| *X*(1) | (Ca) – | O(3) | 2.4382(11) | *Z*(1) | (Al) – | O(1) | 1.8885(9) | *T*(1) | (Si) – | O(1) | 1.6190(10) |
| | | O(5) | 2.3490(12) | | | O(5) | 1.8629(9) | | | O(2) | 1.5885(10) |
| | | O(6) | 2.4625(10) | | | O(9) | 1.9068(9) | | | O(3) | 1.6532(9) |
| | | O(10) | 2.3364(10) | | | O(14) | 1.8608(10) | | | O(4) | 1.6385(10) |
| | | O(13) | 2.3291(9) | | | O(15) | 1.9909(10) | <*T*(1) – O> | | | 1.625 |
| | | O(15) | 2.5879(10) | | | O(16) | 1.9531(10) | *T* volume | | | 2.193(1) |
| <*X*(1) – O> | | | 2.417 | <*Z*(1) – O> | | | 1.911 | λ | | | 1.003 |
| *M* volume | | | 15.545(4) | *M* volume | | | 9.216(2) | σ² | | | 10.5 |
| λ | | | 1.138 | λ | | | 1.006 | | | | |
| σ² | | | 474.6 | σ² | | | 19.4 | *T*(2) | (Si) – | O(4) | 1.6324(10) |
| | | | | | | | | | | O(5) | 1.5987(8) |
| *X*(2) | (Ca) – | O(2) | 2.2909(10) | *Z*(2) | (Al) – | O(7) | 1.9083(9) | | | O(6) | 1.6546(10) |
| | | O(9) | 2.3693(11) | | | O(7) | 1.9197(10) | | | O(7) | 1.6139(10) |
| | | O(9) | 2.4754(10) | | | O(12) | 1.8645(9) | <*T*(2) – O> | | | 1.625 |
| | | O(12) | 2.2439(12) | | | O(13) | 1.9442(9) | *T* volume | | | 2.170(1) |
| | | O(14) | 2.3916(10) | | | O(15) | 1.8692(9) | λ | | | 1.010 |
| | | O(16) | 2.5797(10) | | | O(16) | 1.8833(10) | σ² | | | 37.6 |
| <*X*(2) – O> | | | 2.392 | <*Z*(2) – O> | | | 1.898 | | | | |
| *M* volume | | | 15.467(4) | *M* volume | | | 9.049(2) | *T*(3) | (Si) – | O(8) | 1.6491(10) |
| λ | | | 1.119 | λ | | | 1.005 | | | O(9) | 1.6286(10) |
| σ² | | | 375.5 | σ² | | | 18.5 | | | O(10) | 1.6038(10) |
| | | | | | | | | | | O(11) | 1.6396(9) |
| *Y* | (Fe) – | O(1) | 2.0889(9) | *T*(5) | (B) – | O(3) | 1.4859(14) | <*T*(3) – O> | | | 1.63 |
| | | O(2) | 1.9929(10) | | | O(6) | 1.5296(14) | *T* volume | | | 2.215(1) |
| | | O(6) | 2.3717(10) | | | O(8) | 1.4921(14) | λ | | | 1.003 |
| | | O(8) | 2.1318(9) | | | O(15) | 1.4372(14) | σ² | | | 11.1 |
| | | O(10) | 2.0864(9) | <*T*(5) – O> | | | 1.486 | | | | |
| | | O(14) | 2.7036(10) | *T* volume | | | 1.671(1) | *T*(4) | (Si) – | O(11) | 1.6485(10) |
| <*Y* – O> | | | 2.229 | λ | | | 1.006 | | | O(12) | 1.6041(8) |
| *M* volume | | | 13.305(3) | σ² | | | 25.2 | | | O(13) | 1.6371(10) |
| λ | | | 1.085 | | | | | | | O(14) | 1.6304(10) |
| σ² | | | 224.1 | | | | | <*T*(4) – O> | | | 1.63 |
| | | | | | | | | *T* volume | | | 2.209(1) |
| | | | | | | | | λ | | | 1.004 |
| | | | | | | | | σ² | | | 16.2 |

The distortion parameters λ (the mean quadratic elongation) and σ² (the angular variance) are as defined by Robinson *et al.* (1971).

Similarly, relatively large Mössbauer parameters for $Fe^{2+}$ located at the *Y* site (δ and $\Delta E_Q$, see previous section), indicating a highly irregular site, are in a good accordance with structural evidence of significant distortion of this octahedron (λ and $\sigma^2$, Table 4). Moreover, the *Fe*–O(14) bond in the $YO_6$ octahedron (the longest one at 2.704 Å) is not typical for octahedral coordination of $Fe^{2+}$. In the previous studies, this coordination polyhedron was interpreted as a "significantly distorted" or "irregular" octahedron (see Takéuchi *et al*. 1974, Belokoneva *et al*. 1997, 2001, Andreozzi *et al*. 2000a). However, considering the unusually long *Y*–O(14) bond in all end-members [*Mg*–O(14) = 2.593 Å, manganaxinite: *Mn*–O(14) = 2.68 Å, tinzenite: *Mn*–O(14) = 2.61 Å; Andreozzi *et al*. 2000a, Belokoneva *et al*. 1997, 2001, respectively], the distorted octahedral environment of the *Y*-site cations might be considered as a [5 + 1] coordination rather than the previously reported irregular [6] coordination. Such [5 + 1] coordination has only rarely been reported in the structure of minerals (*e.g.,* in some phosphates, amphiboles and in iron oxides; Chopin *et al*. 2001, Cámara & Oberti 2005, Kelm & Mader 2005, respectively).

On the basis of the stretching frequency of the main OH band in the FTIR spectrum ($\nu$ = 3382 $cm^{-1}$), a bond length of about 2.8 Å from the hydrogen donor oxygen O(16) to the acceptor O(13) can be deduced from the distance–frequency correlation of Libowitzky (1999). This length is in very good agreement with the refined O(16)–H...O(13) distance of 2.7794(13) Å. The refined angle O(16)–H…O(13) is 150.7(19)°, and the (freely) refined O(16)–H bond length is 0.83(2) Å. In order to tentatively explain the additional low-intensity O–H stretching band at *ca.* 3485 $cm^{-1}$ in the FTIR spectrum (Fig. 4), a second possible location of the H atom bonded to O(16) is assumed to be close to the apparent acceptor atom O(6). This position, not previously described from axinite-group minerals, is characterized by the following refined bond-parameters: O(16)–H...O(6) = 3.106 Å, O(16)–H = 0.83 Å, and angle O(16)–H...O(6) = 125.72°.

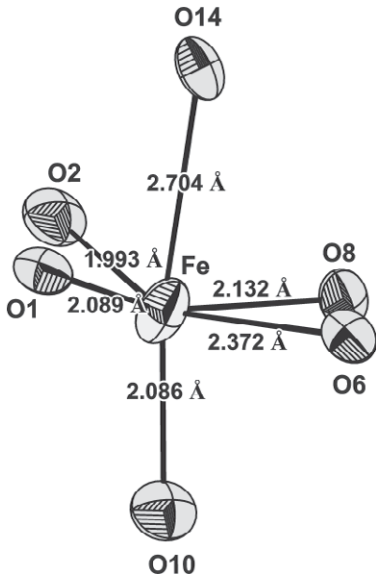


FIG. 5. The distorted $YO_6$ octahedron in the crystal structure of near-end-member ferroaxinite from Malešov (thermal ellipsoids at 99% probability; bond lengths in Å); note the long *Fe*–O(14) bond, suggesting a [5+1] coordination.

### *Crystal-chemical constraints within the axinite group and origin of the ferroaxinite from Malešov*

As was inferred for magnesioaxinite (Novák & Filip 2002), the scarcity of near-end-member ferroaxinite in nature is controlled by the preferred incorporation of the large $Mn^{2+}$ cation at the *Y* site; hence, axinite generally acts as a sink for Mn (Novák & Filip 2002). The presence of smaller divalent cations, Fe and chiefly Mg, at the *Y* site causes the contraction of the whole framework (*cf*. Andreozzi *et al*. 2000a, 2004), and it could control the scarcity of both near-end-member ferroaxinite and magnesioaxinite compositions in nature. At Malešov, a highly iron-contaminated dike of granitic pegmatite cuts magnetite-rich parts of an iron-rich skarn body, where nearly no Mn was available in parental fluids; thus, near-end-member ferroaxinite formed. In addition, the tendency of axinite to form close to end-member compositions at low temperatures, as well as increased miscibility among all end-members at elevated temperatures (Pringle & Kawachi 1980, Grew 1996), probably also played an important role. Our near-end-member ferroaxinite, associated with chlorite and prehnite, formed at relatively low temperature (well below 300°C, Filip 2002) during the late (hydrothermal) stages of pegmatite evolution at Malešov.

## ACKNOWLEDGEMENTS

We are indebted to R. Škoda, B. David, J. Pechoušek, J. Ševčíková and M. Mashlan for technical assistance, to M. Chvátal for providing the ferroaxinite sample, and to G.B. Andreozzi, T. Pilati and R.F. Martin for constructive criticism that significantly improved the manuscript. This work was supported by a Marie Curie Fellowship of the European Commission under contract number HPMT–CT–2000–00138 to JF and by research projects of Ministry of Education of Czech Republic, Grant Nos. MSM6198959218, 1M6198959201 and MSM0021622412. The major part of this work has been done during stay of JF at the University of Vienna.

## REFERENCES

ANDREOZZI, G.B., LUCCHESI, S. & GRAZIANI, G. (2000a): Structural study of magnesioaxinite and its crystal-chemical relations with axinite-group minerals. *Eur. J. Mineral.* **12**, 1185-1194.

ANDREOZZI, G.B., LUCCHESI, S., GRAZIANI, G. & RUSSO, U. (2004): Site distribution of $Fe^{2+}$ and $Fe^{3+}$ in the axinite mineral group: new crystal-chemical formula. *Am. Mineral.* **89**, 1763-1771.

ANDREOZZI, G.B., OTTOLINI, L., LUCCHESI, S., GRAZIANI, G. & RUSSO, U. (2000b): Crystal chemistry of the axinite-group minerals: a multi-analytical approach. *Am. Mineral.* **85**, 698-706.

BASSO, R., DELLA GIUSTA, A. & VLAIC, G. (1973): La structura della tinzenite. *Per. Mineral.* **42**, 369-379.

BEARD, B.L., MEDARIS, L.G., JOHNSON, C.J., MÍSAŘ, Z. & JELÍNEK, E. (1991): Nd and Sr isotope geochemistry of Moldanubian eclogites and garnet peridotites, Bohemian Massif, Czechoslovakia. *Second Eclogite Field Symp., Terra Abstr., Suppl. Terra Nova* **3**, 4.

BELOKONEVA, E.L., GORYUNOVA, A.N., PLETNEV, P.A. & SPIRIDONOV, E.M. (2001): Crystal structure of high-manganese tinzenite from the Falotta deposit in Switzerland. *Crystallogr. Rep.* **46**, 30-32.

BELOKONEVA, E.L., PLETNEV, P.A. & SPIRIDOMOV, E.M. (1997): Crystal structure of low-manganese tinzenite (severginite). *Crystallogr. Rep.* **42**, 934-937.

CÁMARA, F. & OBERTI, R. (2005): The crystal-chemistry of holmquistites: ferroholmquistite from Greenbushes (Western Australia) and hints for compositional constraints in Li–B amphiboles. *Am. Mineral.* **90**, 1167-1176.

CHOPIN, C., FERRARIS, G., PRENCIPE, M., BRUNET, F. & MEDENBACH, O. (2001): Raadeite, $Mg_7(PO_4)_2(OH)_8$: a new dense-packed phosphate from Modum (Norway). *Eur. J. Mineral.* **13**, 319- 327.

DYAR, M.D., TAYLOR, M.E., LUTZ, T.M., FRANCIS, C.A., GUIDOTTI, C.V. & WISE, M. (1998): Inclusive chemical

characterization of tourmaline: Mössbauer study of Fe valence and site occupancy. *Am. Mineral.* **83**, 848-864.

FILIP, J. (2002): *Mineral Assemblages and Chemistry of Axinite from Selected Rocks of the Bohemian Massif*. M.Sc. thesis, Masaryk Univ., Brno, Czech Republic (in Czech).

FUCHS, Y., LINARES, J. & ROBERT, J.L. (1997): Mössbauer and FTIR characterization of a ferro-axinite. *Hyperfine Interact.* **108**, 527-533.

GONSER, U. (1975): Mössbauer spectroscopy in chemistry. *In* Mössbauer Spectroscopy (U. Gonser, ed.). Springer-Verlag, Berlin, Germany (53-96).

GREW, E.S. (1996): Metamorphic borosilicates and boron in metamorphic minerals. *In* Boron: Mineralogy, Petrology and Geochemistry (E.S. Grew & L.M. Anovitz, eds.). *Rev. Mineral. Geochem.* **33**, 387-502.

HENRY, D., BIRCH, W.D. & MACRAE, C. (2005): Manganaxinite from Pyle's limestone near Benambra, and ferroaxinite from Corop, Victoria. *Aust. J. Mineral.* **11**, 27-33.

ITO, T. & TAKÉUCHI, Y. (1952): The crystal structure of axinite. *Acta Crystallogr.* **5**, 202-208.

ITO, T., TAKÉUCHI, Y., OZAWA, T., ARIKI, T., ZOLTAI, T. & FINNEY, S.S. (1969): The crystal structure of axinite revised. *Proc. Jap. Acad.* **45**, 490-494.

JOBBINS, E.A., TRESHAM, A. & YOUNG, B.R. (1975): Pale blue axinite from East Africa. *J. Gemmology* **14**, 368-375.

KACHLÍK, V. (1999): Relationship between Moldanubicum, the Kutná Hora crystalline unit and Bohemicum (central Bohemia, Czech Republic): a result of polyphase Variscan nappe tectonics. *J. Czech Geol. Soc.* **44**, 201-291.

KELM, K. & MADER, W. (2005): Synthesis and structural analysis of $\varepsilon$-$Fe_2O_3$. *Z. Anorg. Allg. Chem.* **631**, 2383-2389.

LIBOWITZKY, E. (1999): Correlation of O–H stretching frequencies and O–H...O hydrogen bond lengths in minerals. *Monatsh. Chem.* **130**, 1047-1059.

LUMPKIN, G.R. & RIBBE, P.H. (1979): Chemistry and physical properties of axinites. *Am. Mineral.* **64**, 635-645.

MASHLAN, M., YEVDOKIMOV, V., PECHOUSEK, J., ZBORIL, R. & KHOLMETSKII, A. (2004): Mössbauer spectrometer with novel moving system and resonant detection of gamma rays. *Hyperfine Interact.* **156**, 15-19.

MCCAMMON, C.A. (2004): Mössbauer spectroscopy: applications. *In* Spectroscopic Methods in Mineralogy (A. Beran & E. Libowitzky, eds.) *Eur. Mineral. Union, Notes in Mineralogy* **6,** 369-398.

MERLET, C. (1994): An accurate computer correction program for quantitative electron-probe microanalysis. *Mikrochim. Acta* **114**, 363-376.

MILTON, C., HILDEBRAND, F.A. & SHERWOOD, A.M. (1953): The identity of tinzenite with manganoan axinite. *Am. Mineral.* **38**, 1148-1158.

NONIUS (2004): COLLECT, *Data Collection Software*. Nonius B.V., Delft, The Netherlands.

NOVÁK, M. & FILIP, J. (2002): Ferroan magnesioaxinite from hydrothermal veins at Lazany, Brno Batholith, Czech Republic. *Neues Jahrb. Mineral., Monatsh.*, 385-399.

NOVÁK, M., SELWAY, J.B., ČERNÝ, P., HAWTHORNE, F.C. & OTTOLINI, L. (1999): Tourmaline of the elbaite–dravite series from an elbaite-subtype pegmatite at Bližná, southern Bohemia, Czech Republic. *Eur. J. Mineral.* **11**, 557-568.

OTWINOWSKI, Z., BOREK, D., MAJEWSKI, W. & MINOR, W. (2003): Multiparametric scaling of diffraction intensities. *Acta Crystallogr.* **A59**, 228-234.

OTWINOWSKI, Z. & MINOR, W. (1997): Processing of X-ray diffraction data collected in oscillation mode. *In* Macromolecular Crystallography **276** (C.V. Carter Jr. & R.M. Sweet, eds.). Academic Press, London, U.K.

OZAKI, M. (1972): Chemical composition and occurrence of axinite. *Kumamoto J. Sci., Geol.* **9**, 1-34.

PEACOCK, M.A. (1937): On the crystallography of axinite and the normal setting of triclinic crystals. *Am. Mineral.* **22**, 588-620.

PIECZKA, A. & KRACZKA, J. (1994): Crystal chemistry of $Fe^{2+}$-axinite from Strzegom. *Mineral. Polonica* **25**, 43-49.

PRINGLE, I.J. & KAWACHI, Y. (1980): Axinite mineral group in low-grade regionally metamorphosed rocks in southern New Zealand. *Am. Mineral.* **65**, 1119-1129.

ROBINSON, K., GIBBS, G.V. & RIBBE, P.H. (1971): Quadratic elongation: a quantitative measure of distorsion in coordination polyhedra. *Science* **172**, 567-570.

SALVIULO, G., ANDREOZZI, G.B. & GRAZIANI, G. (2000): X-ray characterization of Mg, Fe, and Mn natural end-members of the axinite group. *Powder Diffr.* **15**, 180-188.

SANERO, E. & GOTTARDI, G. (1968): Nomenclature and crystal-chemistry of axinite. *Am. Mineral.* **53**, 1407-1411.

SHANNON, R.D. (1976): Revised effective ionic radii and systematic studies of interatomic distances in halides and chalcogenides. *Acta Crystallogr.* **A32**, 751-767.

SHELDRICK, G.M. (1997): SHELXL–97, *a Program for Crystal Structure Refinement*. University of Göttingen, Göttingen, Germany.

SWINNEA, J.S., STEINFINK, H., RENDONDIAZMIRON, L.E. & DELAVEGA, S.E. (1981): The crystal-structure of a Mexican axinite. *Am. Mineral.* **66**, 428-431.

SYNEK, J. & OLIVERIOVÁ, D. (1993): Terrane character of the north-east margin of the Moldanubian zone: the Kutná Hora crystalline complex, Bohemian Massif. *Geol. Rundsch.* **82**, 566-582.

TAKÉUCHI, Y., OZAWA, T., ITO, T., ARAKI, T., ZOLTAI, T. & FINNEY, J.J. (1974): The $B_2Si_8O_{30}$ groups of tetrahedra in axinite and comments on the deformation of Si tetrahedra in silicates. *Z. Kristallogr.* **140**, 289-312.

ZABINSKI, W., PIECZKA, A. & KRACZKA, J. (2002): A Mössbauer study of two axinites from Poland. *Mineral. Polonica* **33**, 27-33.

ŽÁK, T. (2001): Updating of the user-interface fitting program CONFIT to CONFIT2000. *Czech J. Phys.* **51**, 735-742.

*Received December 15, 2005, revised manuscript accepted April 14, 2006.*